

Accepted Manuscript

Improvement of soft magnetic properties for distinctly high Fe content amorphous alloys via longitudinal magnetic field annealing

Hu Li, Aina He, Anding Wang, Lei Xie, Qiang Li, Chengliang Zhao, Guoyang Zhang, Pingbo Chen

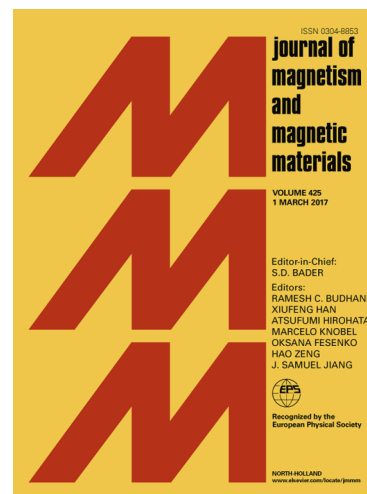
PII: S0304-8853(18)31084-9
DOI: <https://doi.org/10.1016/j.jmmm.2018.09.072>
Reference: MAGMA 64354

To appear in: *Journal of Magnetism and Magnetic Materials*

Received Date: 1 June 2018
Revised Date: 1 August 2018
Accepted Date: 20 September 2018

Please cite this article as: H. Li, A. He, A. Wang, L. Xie, Q. Li, C. Zhao, G. Zhang, P. Chen, Improvement of soft magnetic properties for distinctly high Fe content amorphous alloys via longitudinal magnetic field annealing, *Journal of Magnetism and Magnetic Materials* (2018), doi: <https://doi.org/10.1016/j.jmmm.2018.09.072>

This is a PDF file of an unedited manuscript that has been accepted for publication. As a service to our customers we are providing this early version of the manuscript. The manuscript will undergo copyediting, typesetting, and review of the resulting proof before it is published in its final form. Please note that during the production process errors may be discovered which could affect the content, and all legal disclaimers that apply to the journal pertain.



1 **Improvement of soft magnetic properties for distinctly high Fe content**
2 **amorphous alloys via longitudinal magnetic field annealing**

3 *Hu Li^{1,2}, Aina He^{2,3}, Anding Wang^{2,3*}, Lei Xie^{1,2}, Qiang Li^{1*}, Chengliang Zhao^{2,3},*
4 *Guoyang Zhang², Pingbo Chen².*

5 ¹School of Physics Science and Technology, Xinjiang University, Ürümqi 830046,
6 Xinjiang, China

7 ²Key Laboratory of Magnetic Materials and Devices, Ningbo Institute of Materials
8 Technology and Engineering, Chinese Academy of Sciences, Ningbo 315201, Zhejiang,
9 China

10 ³Zhejiang Province Key Laboratory of Magnetic Materials and Application Technology,
11 Ningbo Institute of Materials Technology and Engineering, Chinese Academy of
12 Sciences, Ningbo 315201, China

13 Corresponding author: Anding Wang and Qiang Li

14 Telephone: +86-574-87617212

15 Fax: +86-574-87617212

16 Email: anding@nimte.ac.cn; qli@xju.edu.cn.

17 **Keywords:** Amorphous alloy; Magnetic field annealing; Soft-magnetic properties;
18 Magnetic domain.

19 **Abstract**

20 The effects of longitudinal magnetic field annealing on soft-magnetic properties (SMPs)
21 and magnetic domain structure of $\text{Fe}_{(82.6-85.7)}\text{Si}_{(2-4.9)}\text{B}_{(9.2-11.2)}\text{P}_{(1.5-2.7)}\text{C}_{0.8}$ amorphous
22 alloys with a distinctly high Fe content of 93.5-95.5 wt.% for high B_s were investigated.
23 It was found that longitudinal magnetic field annealing **could** improve soft-magnetic
24 properties (**SMPs**) of amorphous alloys effectively, except the one with poor thermal

1 stability. Superb magnetic properties containing a minimum coercivity of 0.8 A/m, a
2 maximum effective permeability of 11×10^3 at 1 kHz and minimum core loss of 0.052
3 W/kg (at $B_m = 0.9$ T and $f = 50$ Hz) were successfully obtained. Domain structures were
4 characterized with a Magneto-optical Kerr Microscope to unveil the mechanism of
5 SMPs improvement. Stripe domains were observed in the annealed high Fe content
6 amorphous alloy ribbons with optimal soft magnetic properties.

7 Introduction

8 Fe-based amorphous alloys have aroused worldwide interests from both scientific
9 and technologic aspects due to their excellent soft-magnetic properties (SMPs) [1, 2],
10 and energy saving effect [3]. Further improvements of their] magnetic properties and
11 formability are long-term hot spots, which promote new alloy design theories and
12 preparation techniques [4, 5]. The relatively lower saturation magnetic flux density (B_s)
13 determined by Fe content that compared with silicon steels is the most notable
14 shortcoming and inhabit their wider application [6,7]. Breaking though the Fe content
15 limitation and developing high Fe content amorphous alloys are quite desired, but are
16 difficult. The reported high Fe content alloys have suffered the poor formability and
17 deteriorated soft magnetic properties [8, 9]. In our previous work [10], $\text{Fe}_{(82.6-85.7)}\text{Si}_{(2-}$
18 $4.9)}\text{B}_{(9.2-11.2)}\text{P}_{(1.5-2.7)}\text{C}_{0.8}$ amorphous alloys with a distinctly high Fe content and good
19 manufacturability were successfully developed, which exhibit attractive application
20 prospects if the softness can be improved. Many researchers recently studied the effects
21 of magnetic field annealing on softness of amorphous and nanocrystalline alloys [9, 11-
22 13]. Suzuki et al [12]., investigated the influence of magnetic field annealing on crystal

1 magnetic anisotropy in nanocrystalline soft-magnetic alloys, and found that SMPs
2 could be improved effectively. Zhao et al [13]., studied the effect of longitudinal field
3 annealing on Fe(Co)-based amorphous alloys, and found that SMPs could be improved
4 for the alloys with high Curie temperature (T_c). These studies indicated that magnetic
5 field annealing could promote inner stress release and modulate the domain structure
6 which directly affects the soft-magnetic alloys [12, 14, 15]. However, for the $\text{Fe}_{(82.6-}$
7 $85.7)\text{Si}_{(2-4.9)}\text{B}_{(9.2-11.2)}\text{P}_{(1.5-2.7)}\text{C}_{0.8}$ amorphous alloys with a distinctly high Fe content, the
8 annealing process not only leads to structure relaxation and stress release [13, 16], but
9 also clustering [13, 17-19]. The correlation between magnetic field annealing
10 temperature and SMPs needs further investigation, which have great importance on
11 understanding the structure evolution processes.

12 In this study, the effects of longitudinal magnetic field annealing on SMPs of these
13 high Fe content amorphous alloys were investigated. In order to reveal the correlation
14 between drastically improved SMPs and magnetic structure, magnetic domains were
15 also studied.

16 1. Experimental procedures

17 Amorphous alloy ribbons with nominal compositions (at.%) of $\text{Fe}_{82.7}\text{Si}_{4.9}\text{B}_{9.2}\text{P}_{2.4}\text{C}_{0.8}$,
18 $\text{Fe}_{82.6}\text{Si}_{3.7}\text{B}_{10.9}\text{P}_2\text{C}_{0.8}$, $\text{Fe}_{83.3}\text{Si}_2\text{B}_{11.2}\text{P}_{2.7}\text{C}_{0.8}$, $\text{Fe}_{84.2}\text{Si}_{2.1}\text{B}_{11}\text{P}_{1.9}\text{C}_{0.8}$, and
19 $\text{Fe}_{85.7}\text{Si}_{2.3}\text{B}_{9.7}\text{P}_{1.5}\text{C}_{0.8}$ were prepared by a single Cu roller melt-spinning technique. The
20 ribbon with a width of about 1 mm and a thickness of approximately 25 μm , was cut
21 into 50 mm length for annealing and measurements. The amorphous structure of the as-
22 quenched samples was confirmed by X-ray diffraction (XRD) with Cu $K\alpha$ radiation.

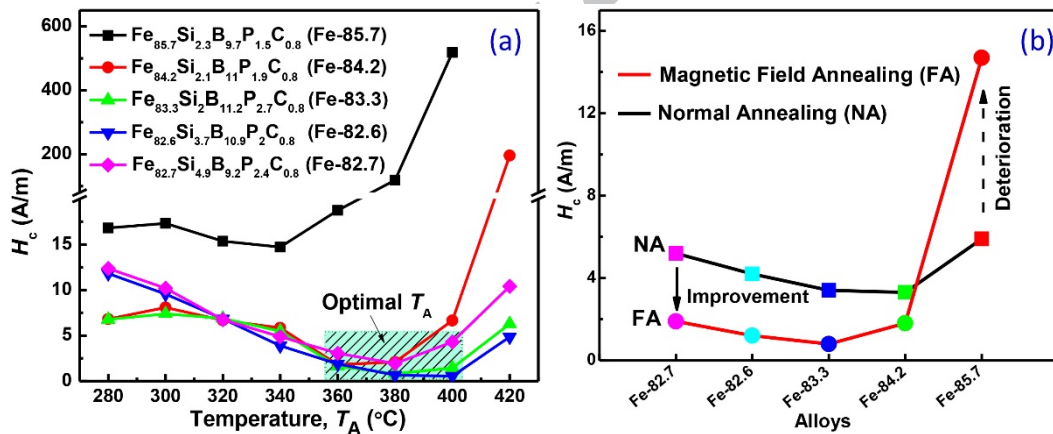
1 Before measuring the magnetic properties, the ribbon samples were annealed at 280-
2 420 °C for 15 min in a vacuum quartz tube with a magnetic field of 1.6×10^3 A/m applied
3 along longitudinal direction (the ribbon axis). The coercivity (H_c) was measured by a
4 DC B-H hysteresis loop tracer under a field of 800 A/m. The measurements of core
5 losses (P) and AC hysteresis loops were carried out by utilizing AC B-H loop tracer
6 under different frequencies of 50, 200 and 1000 Hz, respectively. Permeability (μ_e) at
7 the field of 1 A/m was measured by an impedance analyzer at a frequency range from
8 1 kHz to 10 MHz. The saturation magnetic flux density (B_s) was tested with a vibrating
9 sample magnetometer (VSM) under a maximum applied field of 800 kA/m. Magnetic
10 domain structure of the ribbon samples was observed by using a Magneto-optical Kerr
11 Microscope. All the measurements were carried out at room temperature.

12 2. Results and discussion

13 Fig.1 (a) shows the variation of H_c as a function of annealing temperature (T_A). All
14 the alloys exhibit a similar tendency, i.e., H_c first decreases to a minimum at a T_A
15 (henceforth referred as optimal T_A) and then increases drastically with increasing T_A
16 from 280 °C to 420 °C. The decreases of H_c below optimal T_A can be attributed to the
17 inner stress release during structural relaxation [20]. Besides, the co-effects of magnetic
18 and thermal fields promote the micro-structure uniformity [9, 11], thus improve their
19 SMPs. The increase of H_c over optimal T_A may be ascribed to partial crystallization or
20 clustering, which deteriorate the SMPs due to the formation of hard magnetic phase
21 such as boride and heterogeneous micro-structure with some overgrowth α -Fe grains.

22 Fig. 1 (b) displays the different performance of H_c for $\text{Fe}_{(82.6-85.7)}\text{Si}_{(2-4.9)}\text{B}_{(9.2-11.2)}\text{P}_{(1.5-}$

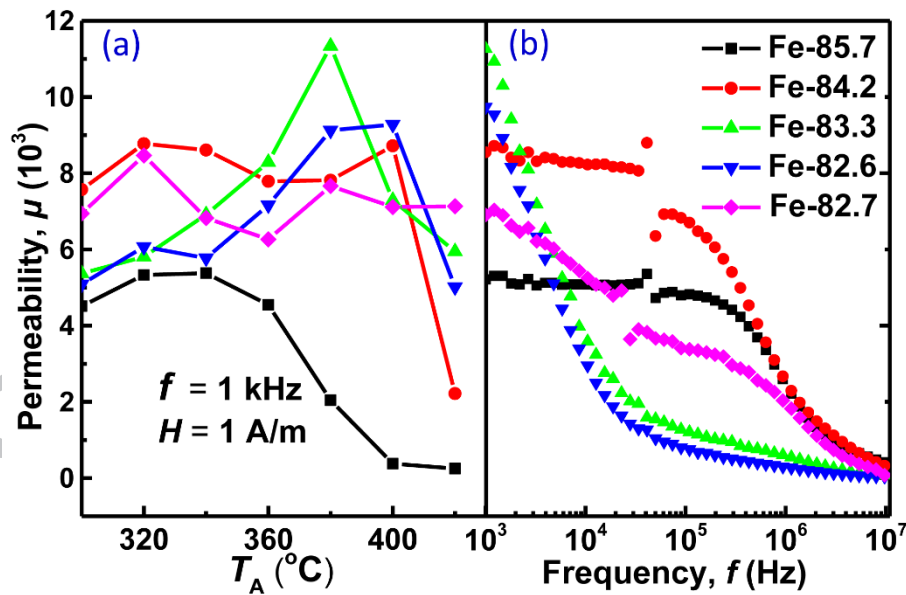
1 $_{2.7}C_{0.8}$ alloys treated by longitudinal magnetic field annealing (FA) and normal
 2 annealing (NA) without magnetic field application, after annealing at optimal T_A . The
 3 H_c of the alloys treated by NA were reported before [10], which were annealed by using
 4 the same furnace. It is clear that the FA can effectively improve the H_c of
 5 $Fe_{82.7}Si_{4.9}B_{9.2}P_{2.4}C_{0.8}$, $Fe_{82.6}Si_{3.7}B_{10.9}P_2C_{0.8}$, $Fe_{83.3}Si_2B_{11.2}P_{2.7}C_{0.8}$ and
 6 $Fe_{84.2}Si_{2.1}B_{11}P_{1.9}C_{0.8}$ alloys. However, for the $Fe_{85.7}Si_{2.3}B_{9.7}P_{1.5}C_{0.8}$ amorphous alloy
 7 with highest Fe content, H_c increases from 5.9 A/m for the NA sample to 14.7 A/m for
 8 the FA sample. It is hence concluded that the FA is not universally effective for all
 9 amorphous alloys.



10
 11 **Fig. 1.** (a) The dependence of H_c on T_A of $Fe_{(82.6-85.7)}Si_{(2-4.9)}B_{(9.2-11.2)}P_{(1.5-2.7)}C_{0.8}$
 12 amorphous alloys treated by longitudinal magnetic field annealing (FA) with an applied
 13 field of 1.6×10^3 A/m and (b) the difference of H_c for FA and normal field-free annealing
 14 (NA) at the optimal T_A .

15 As we know, μ_e is another important parameters of soft-magnetic materials, thus we
 16 also studied the influence of FA on μ_e of $Fe_{(82.6-85.7)}Si_{(2-4.9)}B_{(9.2-11.2)}P_{(1.5-2.7)}C_{0.8}$
 17 amorphous alloys. As shown in Fig. 2 (a), the μ_e at 1 kHz of the present high Fe content
 18 amorphous alloys annealed by FA first increases and then decreases as the T_A increases,

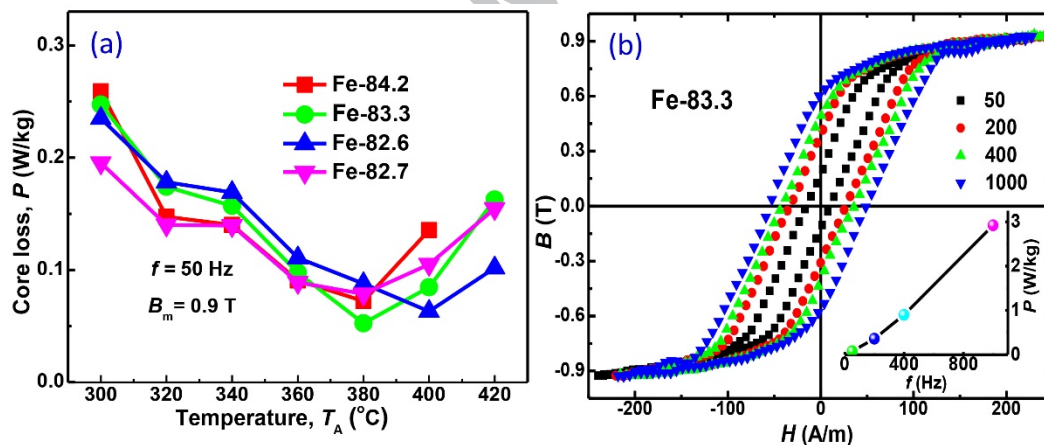
1 and the trend of μ_e with T_A is opposite to that of H_c , as shown in Fig. 1 (a). Compared
 2 with the results of NA samples [3], the μ_e is obviously improved by the method of FA.
 3 For these alloys with improved soft magnetic properties, the optimal μ_e are of quite high
 4 values of $7.8-11 \times 10^3$, which are even better than that of the commercial FeSiB and
 5 FeSiBC alloys [21, 22]. Fig. 2 (b) shows the μ_e of the samples annealed at optimal T_A
 6 as a function of frequency. It is clear that the change tendencies are quite different, i.e.,
 7 the $\text{Fe}_{82.6}\text{Si}_{3.7}\text{B}_{10.9}\text{P}_{2}\text{C}_{0.8}$ and $\text{Fe}_{83.3}\text{Si}_{2}\text{B}_{11.2}\text{P}_{2.7}\text{C}_{0.8}$ alloys exhibit highest μ_e at low f of
 8 about 1 kHz and drastically decreased μ_e at high f , the $\text{Fe}_{84.2}\text{Si}_{2.1}\text{B}_{11}\text{P}_{1.9}\text{C}_{0.8}$ alloy exhibit
 9 attractively high and constant μ_e in large f range of 1-20 kHz. It is hence concluded that
 10 the alloys with FA annealing can has wide application fields.



11
 12 **Fig. 2.** (a) The dependence of effective permeability (μ_e) on T_A at a frequency (f) of 1
 13 kHz and 1 A/m for $\text{Fe}_{(82.6-85.7)}\text{Si}_{(2-4.9)}\text{B}_{(9.2-11.2)}\text{P}_{(1.5-2.7)}\text{C}_{0.8}$ amorphous alloys. (b) The
 14 dependence of effective permeability (μ_e) on f of samples treated by longitudinal FA at
 15 380 $^{\circ}\text{C}$ for 15 min.

16 As shown in Fig. 3 (a), the change of core loss with T_A shows a similar trend to H_c

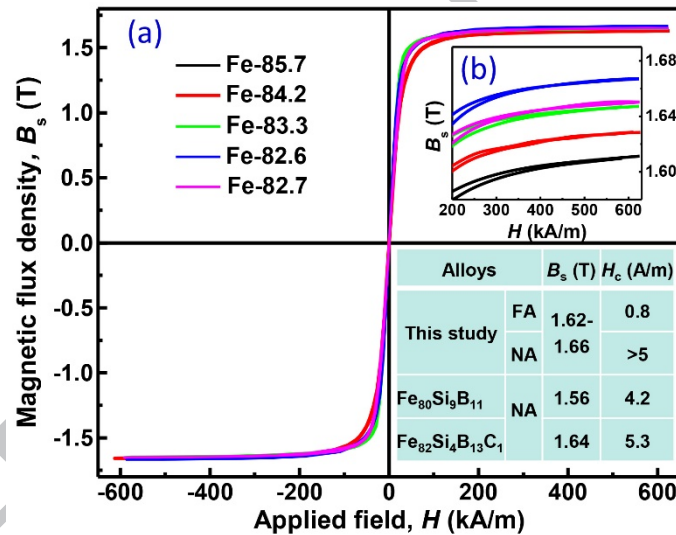
1 for the present amorphous alloys. All alloys exhibit minimum core loss of 0.052-0.1
 2 W/kg at T_A of 380-400 °C and at a frequency of 50 Hz and an induction (B_m) of 0.9 T.
 3 It should be noted that the optimal core loss of the annealed $\text{Fe}_{85.7}\text{Si}_{2.3}\text{B}_{9.7}\text{P}_{1.5}\text{C}_{0.8}$ alloy
 4 is relatively larger than other alloys mentioned above, and thus the results of this alloy
 5 are not included in Fig. 3 (a). The Fig. 3 (b) shows the hysteresis loops measured at
 6 different f of 50, 200, 400 and 1 kHz for the $\text{Fe}_{83.3}\text{Si}_2\text{B}_{11.2}\text{P}_{2.7}\text{C}_{0.8}$ alloy annealed by FA
 7 at optimal T_A . As we can see, the area of hysteresis loop increase smoothly with f
 8 increases from 50 Hz to 1 kHz. The inset of Fig. 3 (b) shows the dependence of core
 9 loss on f . The alloy exhibits extremely low core loss of 0.05-2.9 W/kg in the f range
 10 from 50 Hz to 1 kHz.



11
 12 **Fig. 3.** (a) Core loss as a function of T_A for $\text{Fe}_{(82.6-84.2)}\text{Si}_{(2-4.9)}\text{B}_{(9.2-11.2)}\text{P}_{(1.5-2.7)}\text{C}_{0.8}$
 13 amorphous alloys treated by longitudinal FA, (b) the AC B-H hysteresis loops for the
 14 annealed $\text{Fe}_{83.3}\text{Si}_2\text{B}_{11.2}\text{P}_{2.7}\text{C}_{0.8}$ alloy measured at different frequencies (f).

15 Fig. 4 (a) illustrates the hysteresis loops of the $\text{Fe}_{(82.6-85.7)}\text{Si}_{(2-4.9)}\text{B}_{(9.2-11.2)}\text{P}_{(1.5-2.7)}\text{C}_{0.8}$
 16 amorphous alloys measured with a VSM. As enlarged in inset (b), these high Fe content
 17 alloys exhibit B_s of 1.62-1.66 T. Compared with the results of NA [10], FA has slight
 18 effect on B_s of the present alloys. Since the B_s of the amorphous alloy is mainly depend

1 on the composition and the microstructure of clusters [23], it is speculated that the FA
 2 does not affect the structural phase transition and atomic arrangement. Inset table gives
 3 a comparison of the magnetic properties of the present alloys with different annealing
 4 methods and that of the commercial alloys. It is clear that the high Fe content $\text{Fe}_{(82.6-}$
 5 $85.7)\text{Si}_{(2-4.9)}\text{B}_{(9.2-11.2)}\text{P}_{(1.5-2.7)}\text{C}_{0.8}$ alloys subjected to FA annealing exhibit superb soft
 6 magnetic properties. The longitudinal FA can effectively improve the soft magnetic
 7 properties of these amorphous alloys with distinctly high Fe content, which will
 8 promote the application.



9

10 **Fig. 4.** (a) Hysteresis loops for $\text{Fe}_{(82.6-85.7)}\text{Si}_{(2-4.9)}\text{B}_{(9.2-11.2)}\text{P}_{(1.5-2.7)}\text{C}_{0.8}$ amorphous alloys
 11 subjected to a longitudinal FA. (b) Inset of the partial amplified hysteresis loops. The
 12 insert table shows the B_s and H_c of the present alloys for a normal annealing (NA) and
 13 a magnetic field annealing (FA), as well as the commercial alloys.

14 To sum up, the longitudinal magnetic field annealing is effectively in improving the
 15 SMPs of amorphous alloys with distinctly high Fe content, except the
 16 $\text{Fe}_{85.7}\text{Si}_{2.3}\text{B}_{9.7}\text{P}_{1.5}\text{C}_{0.8}$ alloys with critical Fe content. Superb magnetic properties

1 containing a minimum coercivity of 0.8 A/m, a maximum effective permeability of
2 11×10^3 at 1 kHz and minimum core loss of 0.052 W/kg (at $B_m = 0.9$ T and $f = 50$ Hz)
3 were successfully obtained, which were much better than the commercial alloys. It is
4 of great interests to understand the reasons for the improvement of the SMPs for the
5 four alloys and also the deterioration of the alloy with critical Fe content.

6 First, we identify the magnetic domain structure changes of the two typical
7 $\text{Fe}_{83.3}\text{Si}_2\text{B}_{11.2}\text{P}_{2.7}\text{C}_{0.8}$ and $\text{Fe}_{85.7}\text{Si}_{2.3}\text{B}_{9.7}\text{P}_{1.5}\text{C}_{0.8}$ amorphous alloys. As shown in Fig. 5 (a)
8 and (b), both the AQ and annealed ribbons of $\text{Fe}_{83.3}\text{Si}_2\text{B}_{11.2}\text{P}_{2.7}\text{C}_{0.8}$ alloy exhibit regular
9 shape of stripe magnetic domains. Compared with the irregular branch magnetic
10 domains in AQ sample, the stripe in the annealed sample is much more uniform
11 showing no branches, indicating that the pinning center correlate to the stress and
12 structural heterogeneities. This should be the reason why longitudinal FA can
13 effectively improve the soft magnetic properties by accelerating the internal stress
14 release and modulating the domain structure [11, 12]. However, for the
15 $\text{Fe}_{85.7}\text{Si}_{2.3}\text{B}_{9.7}\text{P}_{1.5}\text{C}_{0.8}$ alloy, irregular magnetic domains with small width are presented
16 in both AQ and annealed samples, as shown in Fig. 6 (c) and (d). Despite the width is
17 more uniform, the domain pattern is occupied with high density of branches, illustrating
18 the strong pinning effect. The domain structure of the four samples are quite consistent
19 with the former SMP changes.

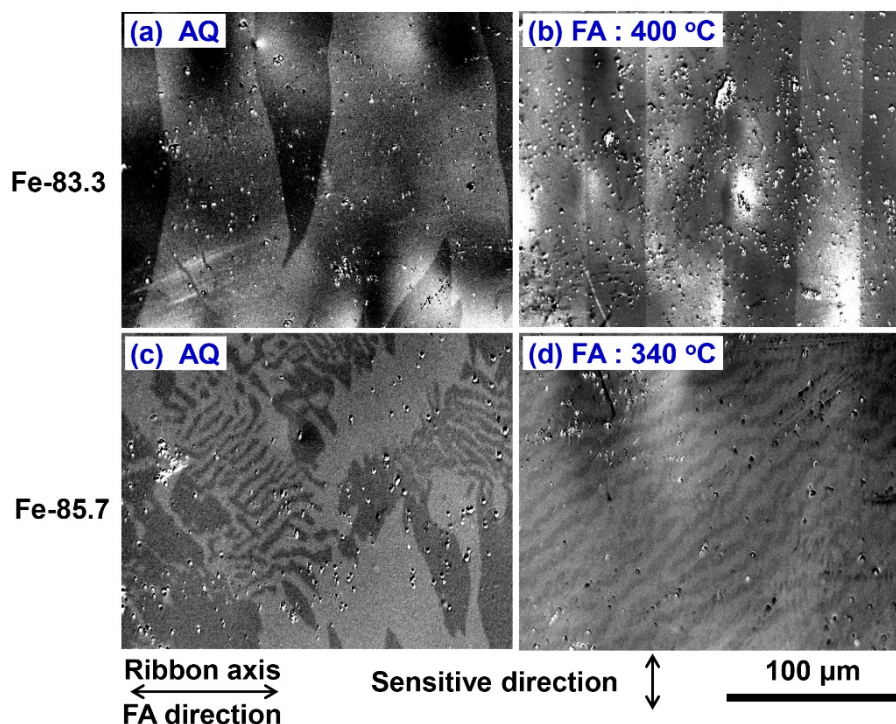
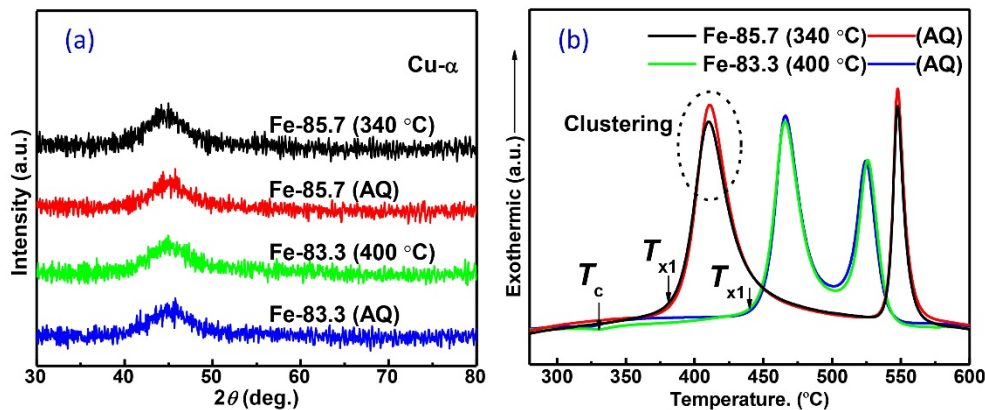


Fig. 5. Images of magnetic domain structures of $\text{Fe}_{83.3}\text{Si}_2\text{B}_{11.2}\text{P}_{2.7}\text{C}_{0.8}$ and $\text{Fe}_{85.7}\text{Si}_{2.3}\text{B}_{9.7}\text{P}_{1.5}\text{C}_{0.8}$ alloy ribbons with different states.

Since the domain structure and soft magnetic properties were mainly depended on the microstructure containing amorphous structure as well as the precipitated phase during annealing [8, 24], we then identified the multiscale change of structure, to reveal the origin of different magnetic performance. X-ray diffraction (XRD) and differential scanning calorimeter (DSC) were performed for the $\text{Fe}_{83.3}\text{Si}_2\text{B}_{11.2}\text{P}_{2.7}\text{C}_{0.8}$ and $\text{Fe}_{85.7}\text{Si}_{2.3}\text{B}_{9.7}\text{P}_{1.5}\text{C}_{0.8}$ alloys. As shown in Fig. 6 (a), no sharp diffraction peaks of crystallization are detected, showing the amorphous structure in XRD resolution for all samples. According to the DSC curves of the four samples shown in the Fig. 6 (b), obvious differences can be found for the two kinds of ribbon samples. The curves of the AQ and annealed $\text{Fe}_{83.3}\text{Si}_2\text{B}_{11.2}\text{P}_{2.7}\text{C}_{0.8}$ samples almost overlap each other. But for the $\text{Fe}_{85.7}\text{Si}_{2.3}\text{B}_{9.7}\text{P}_{1.5}\text{C}_{0.8}$ alloy ribbon annealed at 340 °C, the exothermic peak of the

1 first initial crystallization peak is relatively lower than as-quenched one. This directly
2 proves the drastic clustering of α -Fe which has been reported before [10, 17]. It is well
3 accepted that the good soft magnetic properties of the amorphous alloys are attribute to
4 the uniform microstructure with eliminated free volume and without crystallization or
5 clustering. The narrow temperature interval between the T_c and T_{x1} indicates the poor
6 thermal stability of the $\text{Fe}_{85.7}\text{Si}_{2.3}\text{B}_{9.7}\text{P}_{1.5}\text{C}_{0.8}$ amorphous alloy, which cannot inhibit
7 clustering or crystallization before thorough structure relaxation and stress release. It is
8 noted that the Fe content of the $\text{Fe}_{85.7}\text{Si}_{2.3}\text{B}_{9.7}\text{P}_{1.5}\text{C}_{0.8}$ alloy is closed to the upper limit
9 and critical amorphous forming ability, which means low amorphicity and high density
10 of defects like free volume and clusters of the AQ sample [25]. This is the reason why
11 the AQ sample of $\text{Fe}_{85.7}\text{Si}_{2.3}\text{B}_{9.7}\text{P}_{1.5}\text{C}_{0.8}$ alloy exhibit higher H_c . During the annealing
12 process, the internal stress cannot be thoroughly released and more clusters will formed
13 [17, 26], leading to higher pinning effects and deteriorated soft magnetic properties of
14 $\text{Fe}_{85.7}\text{Si}_{2.3}\text{B}_{9.7}\text{P}_{1.5}\text{C}_{0.8}$ alloy [27]. For other alloys with high thermal stability and large
15 $T_{x1}-T_c$, the AQ samples are of high amorphicity and the structure will homogeneity
16 during the annealing process. It is concluded that the good amorphicity and high thermal
17 stability are essential for excellent soft magnetic properties, no matter what annealing
18 methods are used.



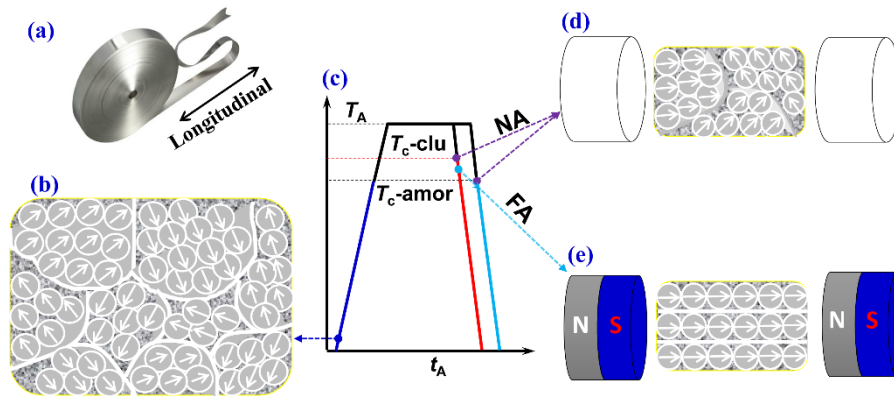
1

2 **Fig. 6.** (a) XRD patterns and (b) DSC curves of $\text{Fe}_{83.3}\text{Si}_2\text{B}_{11.2}\text{P}_{2.7}\text{C}_{0.8}$ and
 3 $\text{Fe}_{85.7}\text{Si}_{2.3}\text{B}_{9.7}\text{P}_{1.5}\text{C}_{0.8}$ alloy ribbons with different states.

4 At last, we proposed a schematic diagram of the domain structure changes during FA
 5 and NA, as shown in Fig. 7 (d) and (e), to simplify the understanding of the
 6 improvement and deterioration of the soft magnetic properties. The applied field
 7 direction is along the axis of ribbon, as shown in Fig. 7 (a). Fig. 7 (b) shows the
 8 magnetic domain structure and the direction of atomic magnetic moments (μ_j) of the
 9 AQ samples. Generally, the variations of domain microstructures can be elucidated
 10 by classical Weiss molecular field theory [28]. According to this theory, the μ_j are parallel
 11 to each other in a domain due to the exchange interaction [29], but the alignment
 12 direction of μ_j varies from domain to domain. It has been reported that the Curie
 13 temperatures of the amorphous alloys ($T_c\text{-amor}$) and α -Fe cluster ($T_c\text{-clu}$) are different
 14 [30], as shown in Fig.7 (c). The $T_c\text{-amor}$ is lower than the annealing temperature (T_A).
 15 The $T_c\text{-clu}$ is higher than the $T_c\text{-amor}$ and will increase with the cluster size and
 16 magnetic interaction. For the $\text{Fe}_{85.7}\text{Si}_{2.3}\text{B}_{9.7}\text{P}_{1.5}\text{C}_{0.8}$ alloy with low thermal stability, the
 17 cluster will grow and the $T_c\text{-clu}$ will be higher than the T_A after annealing. Therefore,
 18 the isothermal annealing process will lead to the precipitation and growth of α -Fe
 19 clusters with high $T_c\text{-clu}$ [17], which will influence the relaxation and inhibit the stress
 20 release of amorphous alloys, and leads to high magnetic anisotropy and bad soft
 21 magnetic properties [31]. During the isothermal annealing process, the alloys with high
 22 thermal stability are in paramagnetic state and the structure relaxation will perform
 23 freely, resulting in high homogeneity and low stress. In the NA cooling stage, the

1 magnetic moments of cluster will return to ferromagnetic state early and preform
2 magnetic domains, leading to induced anisotropy, which is the reason why the alloys
3 with distinctly high Fe content exhibit comparatively worse soft magnetic properties.
4 In the FA cooling stage, the magnetic moments of the cluster and the amorphous will
5 be aligned to the easy magnetization direction by the applied magnetic field, resulting
6 in the great improvement of soft magnetic properties. As studied by Severino [32] and
7 Miguel [33] et al., in Co-based amorphous, the FA treatment substantially increases
8 longitudinal anisotropy and improves the SMPs as it is expected. The magnetization
9 process in longitudinal direction is mainly caused by a displacement of the domain
10 walls. It has also been reported that a large longitudinal anisotropy can increase the
11 magnetic-resonance frequency, which is advantageous for the good permeability-
12 frequency (μ - f) property in the high-frequency region, amplifying the advantage of
13 amorphous alloy in devices with fixed magnetic path like transformer, induction and
14 etc. In a different sense, though, the large anisotropy will lead to rotation of domain
15 walls during magnetization and deteriorated SMPs in the transverse direction. It is
16 hence concluded that the FA treated amorphous alloys are not good for applications in
17 electric motor and other devices with alternating magnetic fields.

18 It should be noted that magnetostriction (λ_s) is also affected by FA and has a critical
19 influence on SMPs. During the annealing of an amorphous alloy, structural relaxation
20 occurs and is accompanied to various degrees by a change in magnetostriction. Ho et
21 al. has proposed that the changes of magnetostriction for Fe-based, FeNi-based and
22 Co-based amorphous alloys are quite different [33]. The influence of FA on the SMPs
23 of the high Fe content amorphous alloys with poor thermal stability should be more
24 complicated and need more investigations.



1
2 **Fig. 7.** (a) Applied field direction along the ribbon axial; (b) A sketch of magnetic
3 domain structures of as-quenched ribbon; (c) Magnetic state of the amorphous alloys
4 and clusters in the annealing process; (d) and (e) are the variation of magnetic moment
5 and domain structure for the annealed ribbon by a normal field-free annealing (NA) and
6 a longitudinal magnetic field annealing (FA), respectively.

7 **3. Conclusions**

8 The effects of longitudinal magnetic field annealing on SMPs of $\text{Fe}_{(82.6-85.7)}\text{Si}_{(2-4.9)}\text{B}_{(9.2-11.2)}\text{P}_{(1.5-2.7)}\text{C}_{0.8}$ amorphous alloys with high Fe content have been investigated
9 and the conclusions are summarized as follows:
10

- 11 1. For the high thermal stability amorphous alloys, longitudinal magnetic field
12 annealing can improve SMPs effectively.
- 13 2. Excellent magnetic properties containing a minimum coercivity of 0.8 A/m, a
14 maximum effective permeability of 11×10^3 at 1 kHz and minimum core loss of 0.052
15 W/kg (at $B_m = 0.9$ T and $f = 50$ Hz) were successfully obtained.
- 16 3. Magnetic domain structure **correlates to** SMPs of amorphous alloys closely. Stripe
17 domain which shows more uniformity at optimal T_A exhibits excellent SMPs.
- 18 4. The magnetic moment of the cluster and the amorphous will be aligned to the easy

1 magnetization direction by the applied longitudinal magnetic field annealing, resulting
2 in the great improvement of soft magnetic properties.

3 **Acknowledgements**

4 This work was supported by the National Key Research and Development Program
5 of China (2017YFB0903902), the National Natural Science Foundation of China (Grant
6 No. 51601206, 51771159, 51771083), and the Zhejiang Provincial Natural Science
7 Foundation (LQ18E010006).

8 **Reference**

- 9 [1] A.D. Wang, C.L. Zhao, A.N. He, H. Men, C. C. Chang, X.M. Wang, Composition design of
10 high B_s Fe-based amorphous alloys with good amorphous-forming ability, *Journal of Alloys*
11 *and Compounds*, 656 (2016) 729-734.
- 12 [2] W.J. Yuan, F.J. Liu, S.J. Pang, Y.J. Song, T. Zhang, Core loss characteristics of Fe-based
13 amorphous alloys, *Intermetallics*, 17 (2009) 278-280.
- 14 [3] N. Zhang, Z. Hu, B. Shen, G. He, Y. Zheng, An integrated source-grid-load planning model at
15 the macro level: Case study for China's power sector, *Energy*, 126 (2017) 231-246.
- 16 [4] J. Xu, Y. Yang, W. Li, Z. Xie, X. Chen, Effect of Si addition on crystallization behavior, thermal
17 ability and magnetic properties in high Fe content Fe-Si-B-P-Cu-C alloy, *Materials Research*
18 *Bulletin*, 97 (2018) 452-456.
- 19 [5] H. Zheng, L. Hu, X. Zhao, C. Wang, Q. Sun, T. Wang, X. Hui, Y. Yue, X. Bian, Poor glass-
20 forming ability of Fe-based alloys: Its origin in high-temperature melt dynamics, *Journal of*
21 *Non-Crystalline Solids*, 471 (2017) 120-127.
- 22 [6] O. Gutfleisch, M.A. Willard, E. Bruck, C.H. Chen, S.G. Sankar, J.P. Liu, Magnetic materials
23 and devices for the 21st century: stronger, lighter, and more energy efficient, *Adv Mater*, 23
24 (2011) 821-842.
- 25 [7] Y. Ogawa, M. Naoe, Y. Yoshizawa and R. Hasegaw, Magnetic properties of high B_s Fe-based
26 amorphous material, *Journal of Magnetism and Magnetic Materials* 304 (2006) E675-E677.
- 27 [8] F. Wang, A. Inoue, Y. Han, S.L. Zhu, F.L. Kong, E. Zanaeva, G.D. Liu, E. Shalaan, F. Al-
28 Marzouki, A. Obaid, Soft magnetic Fe-Co-based amorphous alloys with extremely high
29 saturation magnetization exceeding 1.9 T and low coercivity of 2 A/m, *Journal of Alloys and*
30 *Compounds*, 723 (2017) 376-384.
- 31 [9] H. Zhang, X. Tang, R. Wei, S. Zhu, J. Yang, W. Song, J. Dai, X. Zhu, Y. Sun, Microstructure
32 refinement and magnetization improvement in CoFe thin films by high magnetic field
33 annealing, *Journal of Alloys and Compounds*, 729 (2017) 730-734.
- 34 [10] P. Chen, A. Wang, C. Zhao, A. He, G. Wang, C. Chang, X. Wang, C.-T. Liu, Development of
35 soft magnetic amorphous alloys with distinctly high Fe content, *Science China Physics,*
36 *Mechanics & Astronomy*, 60 (2017).

- 1 [11] V. Zhukova, O.A. Korchuganova, A.A. Aleev, V.V. Tcherdyntsev, M. Churyukanova, E.V.
2 Medvedeva, S. Seils, J. Wagner, M. Ipatov, J.M. Blanco, S.D. Kaloshkin, A. Aronin, G.
3 Abrosimova, N. Orlova, A. Zhukov, Effect of annealing on magnetic properties and structure
4 of Fe-Ni based magnetic microwires, *Journal of Magnetism and Magnetic Materials*, 433 (2017)
5 278-284.
- 6 [12] K. Suzuki, G. Herzer, Magnetic-field-induced anisotropies and exchange softening in Fe-rich
7 nanocrystalline soft magnetic alloys, *Scripta Materialia*, 67 (2012) 548-553.
- 8 [13] C. Zhao, A. Wang, S. Yue, T. Liu, A. He, C. Chang, X. Wang, C.-T. Liu, Significant
9 improvement of soft magnetic properties for Fe(Co)BPSiC amorphous alloys by magnetic field
10 annealing, *Journal of Alloys and Compounds*, 742 (2018) 220-225.
- 11 [14] S. Wen, Y. Ma, D. Wang, Z. Xu, S. Awaji, K. Watanabe, Magnetostriction enhancement by
12 high magnetic field annealing in cast Fe₈₁Ga₁₉ alloy, *Journal of Magnetism and Magnetic
13 Materials*, 442 (2017) 128-135.
- 14 [15] R. Madugundo, O. Geoffroy, T. Waeckerle, B. Frincu, S. Kodjikian, S. Rivoirard, Improved
15 soft magnetic properties in nanocrystalline FeCuNbSiB Nanophy® cores by intense magnetic
16 field annealing, *Journal of Magnetism and Magnetic Materials*, 422 (2017) 475-478.
- 17 [16] X. Li, J. Liu, C. Qu, K. Song, L. Hu, L. Wang, Preparation and properties of FeBP Sn soft
18 magnetic amorphous alloys with Fe contents higher than 83%, *Journal of Non-Crystalline
19 Solids*, 469 (2017) 27-30.
- 20 [17] P. Chen, T. Liu, F. Kong, A. Wang, C. Yu, G. Wang, C. Chang, X. Wang, Ferromagnetic
21 element microalloying and clustering effects in high B_s Fe-based amorphous alloys, *Journal of
22 Materials Science & Technology*, (2017).
- 23 [18] F. Chen, T. Zhang, J. Wang, L. Zhang, G. Zhou, Investigation of domain wall pinning effect
24 induced by annealing stress in sintered Nd-Fe-B magnet, *Journal of Alloys and Compounds*,
25 640 (2015) 371-375.
- 26 [19] C. Zhao, A. Wang, A. He, S. Yue, C. Chang, X. Wang, R.-W. Li, Correlation between soft-
27 magnetic properties and $T_{x1}-T_c$ in high B_s FeCoSiBPC amorphous alloys, *Journal of Alloys and
28 Compounds*, 659 (2016) 193-197.
- 29 [20] J.S. Blázquez, J. Marcin, F. Andrejka, V. Franco, A. Conde, I. Skorvanek, Anisotropy field
30 distribution in soft magnetic Hitperm alloys submitted to different field annealing processes,
31 *Journal of Alloys and Compounds*, 658 (2016) 367-371.
- 32 [21] Z. Li, Y. Dong, S. Pauly, C. Chang, R. Wei, F. Li, X.-M. Wang, Enhanced soft magnetic
33 properties of Fe-based amorphous powder cores by longitude magnetic field annealing, *Journal
34 of Alloys and Compounds*, 706 (2017) 1-6.
- 35 [22] E.A. Périgo, S. Nakahara, Y. Pittini-Yamada, Y. de Hazan, T. Graule, Magnetic properties of
36 soft magnetic composites prepared with crystalline and amorphous powders, *Journal of
37 Magnetism and Magnetic Materials*, 323 (2011) 1938-1944.
- 38 [23] A.D. Wang, H. Men, B.L. Shen, G.Q. Xie, A. Makino, A. Inoue, Effect of P on crystallization
39 behavior and soft-magnetic properties of Fe_{83.3}Si₄Cu_{0.7}B_{12-x}P_x nanocrystalline soft-magnetic
40 alloys, *Thin Solid Films*, 519 (2011) 8283-8286.
- 41 [24] J. Fornell, S. González, E. Rossinyol, S. Suriñach, M.D. Baró, D.V. Louzguine-Luzgin, J.H.
42 Perepezko, J. Sort, A. Inoue, Enhanced mechanical properties due to structural changes
43 induced by devitrification in Fe-Co-B-Si-Nb bulk metallic glass, *Acta Materialia*, 58 (2010)
44 6256-6266.

- 1 [25] C. Fan, C.T. Liu, G. Chen, P.K. Liaw, Quantitatively defining free-volume, interconnecting-
2 zone and cluster in metallic glasses, *Intermetallics*, 57 (2015) 98-100.
- 3 [26] D.V. Gunderov, E.V. Boltynjuk, E.V. Ubyivovk, A.V. Lukyanov, A.A. Churakova, A.R.
4 Kilmametov, Y.S. Zamula, R.Z. Valiev, Cluster structure in amorphous Ti-Ni-Cu alloys
5 subjected to high-pressure torsion deformation, *Journal of Alloys and Compounds*, 749 (2018)
6 612-619.
- 7 [27] B. Zang, R. Parsons, K. Onodera, H. Kishimoto, A. Kato, A.C.Y. Liu, K. Suzuki, Effect of
8 heating rate during primary crystallization on soft magnetic properties of melt-spun Fe-B alloys,
9 *Scripta Materialia*, 132 (2017) 68-72.
- 10 [28] Augusto Visintin, A Weiss-type model of ferromagnetism. *Physica B* 275 (2000) 87-91
- 11 [29] M. Soderžnik, H. Sepehri-Amin, T.T. Sasaki, T. Ohkubo, Y. Takada, T. Sato, Y. Kaneko, A.
12 Kato, T. Schrefl, K. Hono, Magnetization reversal of exchange-coupled and exchange-
13 decoupled Nd-Fe-B magnets observed by magneto-optical Kerr effect microscopy, *Acta*
14 *Materialia*, 135 (2017) 68-76.
- 15 [30] S. Kaloshkin, M. Churyukanova, V. Zadorozhnyi, I. Shchetinin, R.K. Roy, Curie temperature
16 behaviour at relaxation and nanocrystallization of Finemet alloys, *Journal of Alloys and*
17 *Compounds*, 509 (2011) S400-S403.
- 18 [31] A. Gavrilović, L.D. Rafailović, D.M. Minić, J. Wosik, P. Angerer, D.M. Minić, Influence of
19 thermal treatment on structure development and mechanical properties of amorphous
20 $Fe_{73.5}Cu_1Nb_3Si_{15.5}B_7$ ribbon, *Journal of Alloys and Compounds*, 509 (2011) S119-S122.
- 21 [32] A. M. Severino, , A. D. Santos, E. P. Missell, Changes in induced anisotropy and
22 magnetostriction in co-based amorphous-alloys, *Journal of Magnetism and Magnetic Materials*,
23 96 (1991) 167-174.
- 24 [33] C. Miguel, , A. P. Zhukov, J. J. del Val, A. R. de Arellano, J. Gonzalez, Effect of stress and/or
25 field annealing on the magnetic behavior of the $(Co_{77}Si_{13.5}B_{9.5})(90)Fe_7Nb_3$ amorphous
26 alloy, *Journal of Applied Physics*, 97 (2005) 8.
- 27 [33] Ho, K. Y., F. Xu and X. Y. Xiong, Effects of magnetic and stress annealing on the change in
28 magnetostriction for magnetically soft amorphous-alloys, *Journal of Magnetism and Magnetic*
29 *Materials* 119 (1993) 318-320.